
Adversarial Fisher Vectors for Unsupervised Representation Learning

Shuangfei Zhai Walter Talbott Carlos Guestrin Joshua M. Susskind
Apple Inc.
{szhai, wtalbott, guestrin, jsusskind}@apple.com

Abstract

We examine Generative Adversarial Networks (GANs) through the lens of deep Energy Based Models (EBMs), with the goal of exploiting the density model that follows from this formulation. In contrast to a traditional view where the discriminator learns a constant function when reaching convergence, here we show that it can provide useful information for downstream tasks, e.g., feature extraction for classification. To be concrete, in the EBM formulation, the discriminator learns an unnormalized density function (i.e., the negative energy term) that characterizes the data manifold. We propose to evaluate both the generator and the discriminator by deriving corresponding Fisher Score and Fisher Information from the EBM. We show that by assuming that the generated examples form an estimate of the learned density, both the Fisher Information and the normalized Fisher Vectors are easy to compute. We also show that we are able to derive a distance metric between examples and between sets of examples. We conduct experiments showing that the GAN-induced Fisher Vectors demonstrate competitive performance as unsupervised feature extractors for classification and perceptual similarity tasks. Code is available at <https://github.com/apple/ml-afv>.

1 Introduction

Generative adversarial networks (GANs) [1] are state-of-the-art generative modeling methods, where a discriminator network is jointly trained with a generator network to solve a minimax game. According to the original theory in [1], the discriminator reduces to a constant function that assigns a score of 0.5 everywhere when Nash Equilibrium is reached, making the discriminator useless for anything beyond training the generator. Moreover, the generator models the data density, but in an implicit form that precludes its application to scenarios where an explicit density estimate would be useful. Recently, [2, 3, 4] show that training an energy-based model (EBM) with a parameterized variational distribution reduces to a similar minimax GAN game. This EBM view, in contrast to the original GAN formulation, leads to an interpretation where the discriminator itself is an explicit density model of the data.

We show that under certain approximations, the deep EBMs can be trained with a modern GAN implementation (see Sec. 2.2). We then focus on exploring the utility of the density models learned according to the EBM interpretation. Inspired by the approach in [5], we show how to use the Fisher Score and Fisher Information induced by the learned density model to compute representations of data samples. Namely, we derive normalized Fisher Vectors and Fisher Distance measure to estimate similarities both between individual data samples and between sets of samples. We call these derived representations Adversarial Fisher Vectors (AFVs).

We propose to apply the density model and derived AFV representation in several ways. First, we show that the learned AFV representations are useful as pre-trained features for linear classification tasks, and that the similarity function induced by the learned density model can be used as a perceptual

metric that correlates well with human judgments. Second, we show that estimating similarities between sets using AFV allows us to monitor the training process. Notably, we show that the Fisher Distance between the set of validation examples and generated examples can effectively capture the notion of overfitting, which is verified by the quality of the corresponding AFVs.

As an additional benefit of the EBM interpretation, we provide a view of the generator update as an approximation to stochastic gradient Markov Chain Monte Carlo (MCMC) sampling [6], similar to [4]. We show that directly enforcing local updates of the generated examples improves training stability, especially early in training.

By fully utilizing the density model derived from the EBM framework, we make the following contributions:

- AFV representations are derived for unsupervised feature extraction and similarity estimation from the learned density model.
- GAN training is improved through monitoring (AFV metrics) and stability (MCMC updates).
- AFV is shown to be useful for extracting unsupervised features, leading to state-of-the-art performance on classification and perceptual similarity benchmarks.

2 Background

2.1 Generative Adversarial Networks

GANs [1] learn a discriminator and generator network simultaneously by solving a minimax game:

$$\max_G \min_D \mathbb{E}_{\mathbf{x} \sim p_{data}(\mathbf{x})} [-\log D(\mathbf{x})] - \mathbb{E}_{\mathbf{z} \sim p_{\mathbf{z}}(\mathbf{z})} [\log(1 - D(G(\mathbf{z})))] \tag{1}$$

where $p_{data}(\mathbf{x})$ denotes the data distribution; $D(\mathbf{x})$ is the discriminator that takes as input a sample and outputs a scalar in $[0, 1]$; $G(\mathbf{z})$ is the generator that maps a random vector $\mathbf{z} \in R^d$ drawn from a pre-defined distribution $p(\mathbf{z})$. Equation 1 suggests a training procedure consisting of two loops: in the inner loop D is trained until convergence given G , and in the outer loop G is updated one step given D . [1] shows that GANs implicitly minimize the Jensen-Shannon divergence between the generator distribution $p_G(\mathbf{x})$ and the data distribution $p_{data}(\mathbf{x})$, and hence samples from G approximate the true data distribution when the minimax game reaches Nash Equilibrium.

2.2 GANs as variational training of deep EBMs

Following [3], let an EBM define a density function as: $p_E(\mathbf{x}) = \frac{e^{-E(\mathbf{x})}}{\int_{\mathbf{x}} e^{-E(\mathbf{x})} d\mathbf{x}}$, where $E(\mathbf{x})$ is the energy of input \mathbf{x} . We can then write its negative log likelihood (NLL) as: $\mathbb{E}_{\mathbf{x} \sim p_{data}(\mathbf{x})} [E(\mathbf{x})] + \log[\int_{\mathbf{x}} e^{-E(\mathbf{x})} d\mathbf{x}]$, which can be further developed as:

$$\begin{aligned} \mathbb{E}_{\mathbf{x} \sim p_{data}(\mathbf{x})} [E(\mathbf{x})] + \log \int_{\mathbf{x}} q(\mathbf{x}) \frac{e^{-E(\mathbf{x})}}{q(\mathbf{x})} d\mathbf{x} &= \mathbb{E}_{\mathbf{x} \sim p_{data}(\mathbf{x})} [E(\mathbf{x})] + \log \mathbb{E}_{\mathbf{x} \sim q(\mathbf{x})} \left[\frac{e^{-E(\mathbf{x})}}{q(\mathbf{x})} \right] \\ &\geq \mathbb{E}_{\mathbf{x} \sim p_{data}(\mathbf{x})} [E(\mathbf{x})] + \mathbb{E}_{\mathbf{x} \sim q(\mathbf{x})} \left[\log \frac{e^{-E(\mathbf{x})}}{q(\mathbf{x})} \right] = \mathbb{E}_{\mathbf{x} \sim p_{data}(\mathbf{x})} [E(\mathbf{x})] - \mathbb{E}_{\mathbf{x} \sim q(\mathbf{x})} [E(\mathbf{x})] + H(q), \end{aligned} \tag{2}$$

where $q(\mathbf{x})$ is an auxiliary distribution which we call the *variational distribution*, with $H(q)$ denoting its entropy. Equation 2 is a straightforward application of Jensen’s inequality, and it gives a variational lower bound on the NLL given $q(\mathbf{x})$. The lower bound is tight when $\frac{e^{-E(\mathbf{x})}}{q(\mathbf{x})}$ is a constant w.r.t. \mathbf{x} , i.e., $q(\mathbf{x}) \propto e^{-E(\mathbf{x})}$, $\forall \mathbf{x}$, which implies that $q(\mathbf{x}) = p_E(\mathbf{x})$. We then let $D(\mathbf{x}) = -E(\mathbf{x})$ and $q(\mathbf{x}) = p_G(\mathbf{x})$ (i.e., the implicit distribution defined by a generator as in GANs), which leads to an objective as follows:

$$\min_D \max_G \mathbb{E}_{\mathbf{x} \sim p_{data}(\mathbf{x})} [-D(\mathbf{x})] + \mathbb{E}_{\mathbf{z} \sim p_{\mathbf{z}}(\mathbf{z})} [D(G(\mathbf{z}))] + H(p_G), \tag{3}$$

where in the inner loop, the variational lower bound is maximized w.r.t. p_G ; the energy model then is updated one step to decrease the NLL with the optimal p_G (see Figure 1).



Figure 1: EBM view of GAN, in which the generator is first updated such that sampling from $P_G(\mathbf{x})$ approximates the discriminator distribution $P_D(\mathbf{x})$; the discriminator is then updated to fit $P_D(\mathbf{x})$ to $P_{data}(\mathbf{x})$.

Equation 3 and Equation 1 bear a lot of similarity, both taking the form of a minimax game between D and G . The three notable differences, however, are 1) the emergence of the entropy regularization term $H(p_G)$ in Equation 3 which in theory prevents the generator from collapsing¹, 2) the order of optimizing D and G , and 3) D is a density model for the data distribution and G learns to sample from D .

In practice, it is difficult to come up with a differentiable approximation to the entropy term $H(p_G)$. We instead rely on implicit regularization methods such as using Batch Normalization [8] on the generator (see Sec. 3.2 for more analysis). This simplification makes it possible to implement Equation 3 in exactly the same way as a GAN, where D and G are alternately updated on a few mini-batches of data. We can then borrow the implementation of a state-of-the-art GAN, and focus on utilizing the trained model as discussed below.

3 Methodology

3.1 Adversarial Fisher Vectors

In the EBM view of GANs, the discriminator is a dual form of the generator, where in the perfect scenario each defines a distribution that matches the training data. By nature, interpreting the generator distribution can be easily done by first sampling from it, and inspecting the quality of samples produced. However, it is not clear how to evaluate or use a discriminator, even under the assumption that it captures as much information about the training data as the generator does. To this end, we turn our eye to the theory of Fisher Information [5, 9], starting by adopting the EBM view of GANs as discussed before.

Given a density model $p_\theta(\mathbf{x})$, with $\mathbf{x} \in R^d$ as the input and θ being the model parameters, we can derive the Fisher Score of an example \mathbf{x} is as $U_{\mathbf{x}} = \nabla_\theta \log p_\theta(\mathbf{x})$. Intuitively, the Fisher Score encodes the desired change of model parameters to better fit the example \mathbf{x} . We further define the Fisher Information as $\mathcal{I} = \mathbb{E}_{\mathbf{x} \sim p_\theta(\mathbf{x})} [U_{\mathbf{x}} U_{\mathbf{x}}^T]$. According to information geometry theory [10], the generative model defines a local Riemannian manifold, over model parameters θ , with a local metric given by the Fisher Information. Following [5], one can then use the Fisher Score to map an example \mathbf{x} to the model space, and measure the proximity between two examples \mathbf{x}, \mathbf{y} by $U_{\mathbf{x}}^T \mathcal{I}^{-1} U_{\mathbf{y}}$. One can also naturally adopt the same principle to induce a distance metric as $\mathcal{D}(\mathbf{x}, \mathbf{y}) = (U_{\mathbf{x}} - U_{\mathbf{y}})^T \mathcal{I}^{-1} (U_{\mathbf{x}} - U_{\mathbf{y}})$, which we call the Fisher Distance. Additionally, we can generalize the notion of Fisher Distance to take two sets of examples as input:

$$\mathcal{D}(\mathbf{X}, \mathbf{Y}) = \left(\frac{1}{|\mathbf{X}|} \sum_{\mathbf{x} \in \mathbf{X}} U_{\mathbf{x}} - \frac{1}{|\mathbf{Y}|} \sum_{\mathbf{y} \in \mathbf{Y}} U_{\mathbf{y}} \right)^T \mathcal{I}^{-1} \left(\frac{1}{|\mathbf{X}|} \sum_{\mathbf{x} \in \mathbf{X}} U_{\mathbf{x}} - \frac{1}{|\mathbf{Y}|} \sum_{\mathbf{y} \in \mathbf{Y}} U_{\mathbf{y}} \right).$$

We finally define the AFV of an example as:

$$V_{\mathbf{x}} = \mathcal{I}^{-\frac{1}{2}} U_{\mathbf{x}},$$

so the Fisher Distance is equivalent to the Euclidean distance with AFVs.

AFVs provide a valuable tool for utilizing a generative model. Given a fixed model, two examples are considered identical only if the desired change to the model parameters are the same. As a simple illustration, for a standard Gaussian distribution $\mathcal{N}(\mu, \sigma)$, two examples $x_1 = \mu + 1$ and $x_2 = \mu - 1$ have exactly the same density, but still have different Fisher Scores. As a matter of fact, classical

¹Interestingly, similar diversity promoting regularization terms have been independently explored in the GAN literature, such as in [7].

Fisher Vectors have successfully been applied by utilizing relatively simple density models such as Mixture of Gaussians, see [11] for detailed examples.

In the context of EBMs, we parameterize the density model in intervals of D as $p_\theta(\mathbf{x}) = \frac{e^{D(\mathbf{x};\theta)}}{\int_{\mathbf{x}} e^{D(\mathbf{x};\theta)} d\mathbf{x}}$ with θ explicitly being the parameters of D . We then derive the Fisher Score as

$$U_{\mathbf{x}} = \nabla_{\theta} D(\mathbf{x}; \theta) - \nabla_{\theta} \log \int_{\mathbf{x}} e^{D(\mathbf{x};\theta)} d\mathbf{x} = \nabla_{\theta} D(\mathbf{x}; \theta) - \mathbb{E}_{\mathbf{x} \sim p_{\theta}(\mathbf{x})} \nabla_{\theta} D(\mathbf{x}; \theta). \quad (4)$$

According to Equation 3, the EBM interpretation of a GAN entails that during training, the generator is updated to match the distribution $p_G(\mathbf{x})$ to $p_\theta(\mathbf{x})$. This allows us to conveniently approximate the second term by sampling from the generator’s distribution, resulting in the Fisher Score and Fisher Information we work with:

$$U_{\mathbf{x}} = \nabla_{\theta} D(\mathbf{x}; \theta) - \mathbb{E}_{\mathbf{z} \sim p(\mathbf{z})} \nabla_{\theta} D(G(\mathbf{z}); \theta), \quad \mathcal{I} = \mathbb{E}_{\mathbf{z} \sim p(\mathbf{z})} [U_{G(\mathbf{z})} U_{G(\mathbf{z})}^T]. \quad (5)$$

By approximating the density model defined by D with the learned generator distribution, we have come up with a scalable approximation to the Fisher Score and Fisher Information for an un-normalized deep density model. In particular, the Fisher Score takes the form of the gradient of the discriminator (the negative energy in EBM terms) output w.r.t. its parameters, subtracted by the average gradient of all generated examples. The Fisher Information, on the other hand, elegantly reduces to the covariance matrix of the gradient of the generated examples.

For practical settings where D takes the form of a deep convolutional neural network, directly computing the AFVs can be expensive, as the vectors can easily be up to millions of dimensions. We thus resort to a diagonal approximation of the Fisher Information, which yields an efficient form of the AFV:

$$V_{\mathbf{x}} = (\text{diag}(\mathcal{I})^{-\frac{1}{2}}) U_{\mathbf{x}}, \quad (6)$$

where \mathcal{I} and $U_{\mathbf{x}}$ are as defined in Equation 5, and diag denotes the diagonal matrix operator.

3.2 Generator update as stochastic gradient MCMC

The use of a generator provides an efficient way of drawing samples from the EBM. However, in practice, great care needs to be taken to make sure that G is well conditioned to produce examples that cover enough modes of D . There is also a related issue where the parameters of G will occasionally undergo sudden changes, generating samples drastically different from iteration to iteration, which contributes to training instability and lower model quality.

In light of these issues, we provide a different treatment of G , borrowing inspirations from the Markov Chain Monte Carlo (MCMC) literature. MCMC variants have been widely studied in the context of EBMs, which can be used to sample from an unnormalized density and approximate the partition function [12, 13]. Stochastic gradient MCMC [6] is of particular interest as it utilizes the gradient of the log probability w.r.t. the input, and performs gradient ascent to incrementally update the samples (while adding noise to the gradients). See [14] for a recent application of this technique to deep EBMs. We speculate that it is possible to train G to mimic the the stochastic gradient MCMC update rule, such that the samples produced by G will approximate the true model distribution.

To be concrete, we want to constrain the G updates to be local w.r.t. the generated examples, similar to one step stochastic gradient MCMC sampling. To do this, We maintain an old copy of G denoted as \tilde{G} (e.g., obtained by Polyak averaging of G parameters) and let the G objective be: $\min_G \mathbb{E}_{\mathbf{z} \sim p(\mathbf{z})} [\frac{1}{2} \|G(\mathbf{z}) - \tilde{G}(\mathbf{z}) + \lambda \epsilon\|^2 - \frac{\lambda}{2} D(G(\mathbf{z}))]$. Here $\lambda \in R^+$ is a small scalar quantity that corresponds to the step size of the stochastic gradient MCMC update, $\epsilon \sim \mathcal{N}(0, \mathcal{I})$ is white Gaussian noise. It is not hard to see that the non-parametric local minimum for Equation 7 w.r.t. $G(\mathbf{z})$ is $G(\mathbf{z}) = \tilde{G}(\mathbf{z}) + \frac{\lambda}{2} \nabla_{\mathbf{x}} D(\mathbf{x})|_{\mathbf{x}=\tilde{G}(\mathbf{z})} + \lambda \epsilon$, which corresponds to one step of stochastic gradient MCMC update, where the starting point is given by $\tilde{G}(\mathbf{z})$. In practice, we can optionally ignore the ϵ term; we can also adopt the same principle to any loss variants such as hinge loss [15], or squared loss, which gives us a generalized form of the MCMC objective:

$$\min_G \mathbb{E}_{\mathbf{z} \sim p(\mathbf{z})} [L(D(G(\mathbf{z}))) + \gamma \|G(\mathbf{z}) - \tilde{G}(\mathbf{z})\|^2], \quad (7)$$

where L denotes a loss function and $\gamma \in R^+$ is a weight factor. Note that this explicit regularization is not always necessary in the sense that the local update can also be implicitly achieved via careful

architecture design and training scheduling. However, we have found that including this term can effectively reduce the mode collapse problem and increase training stability, especially early in training where G undergoes large gradients. This MCMC inspired objective is also similar to the historical averaging trick proposed in [7], but with the importance distinction that we constrain the locality of updates in the sample space, rather than the parameter space.

4 Related Work

A number of GAN variants have been proposed by extending the notion of discriminator to a critic that measures the discrepancy of two distributions, with notable examples including Wasserstein GAN [16], f-GAN [17], MMD-GAN [18]. Of particular interest to this work is the connection between GANs and deep energy-based models (EBMs) [19]. It is shown that the training procedure of a GAN resembles that of a deep EBM with variational inference [2, 3, 4, 15]. Our work differs from these in the sense that we directly utilize the discriminator by taking advantage of the fact that it learns a density model of data. There has also been an increasing in the interest of deep EBMs trained with traditional sampling approaches, see [20, 21]. Our implementation of EBMs has the benefit of directly learning a parameterized sampler, which is more efficient than iterative MCMC based sampling approaches.

Other works have introduced techniques to improve GAN stability using regularization techniques such as adding noise [22], gradient penalization [23], or conditioning the weights with spectral normalization [24]. Mode collapse has been tackled by encouraging the model to generate high entropy samples [7] and by introducing new training formulations [16]. These techniques are typically adhoc and lack a formal justification. We show a particular connection of our MCMC based G update rule to the the gradient penalty line of work as in [23, 25]. To see this, instead of always sampling from the generator, we allow a small probability ρ to sample particles starting from a real example \mathbf{x} . Plugging this in the D objective, we obtain:

$$\begin{aligned} & \min_D \mathbb{E}_{\mathbf{x} \sim p_{data}(\mathbf{x})} [-D(\mathbf{x})] + (1 - \rho) \mathbb{E}_{\mathbf{z} \sim p_{\mathbf{z}}(\mathbf{z})} [D(G(\mathbf{z}))] - \\ & \quad \rho \mathbb{E}_{\mathbf{x} \sim p_{data}(\mathbf{x})} [-D(\mathbf{x} + \frac{\lambda}{2} \nabla_{\mathbf{x}} D(\mathbf{x}) + \lambda \epsilon)] \\ & \approx \min_D \mathbb{E}_{\mathbf{x} \sim p_{data}(\mathbf{x})} [-(1 - \rho) D(\mathbf{x})] + (1 - \rho) \mathbb{E}_{\mathbf{z} \sim p_{\mathbf{z}}(\mathbf{z})} [D(G(\mathbf{z}))] + \\ & \quad \frac{\rho \lambda}{2} \mathbb{E}_{\mathbf{x} \sim p_{data}(\mathbf{x})} \|\nabla_{\mathbf{x}} D(\mathbf{x})\|^2, \end{aligned}$$

which is exactly the zero centered gradient penalty regularization proposed in [25].

In early work incorporating generative models into discriminative classifiers, [5] showed that one can use Fisher Information to derive a measure of the similarity between examples. [11] extended this work by introducing the Fisher Vector representation for image classification using Gaussian mixture models for density modeling. More recently, Fisher Information has also been applied to tasks such as meta learning [26]. In this work, we show that it is possible to extend this idea to state-of-the-art deep generative models. In particular, by utilizing the generator as a learned sampler from the density model, we are able to overcome the difficulty of computing the Fisher Information from an un-normalized density model. Compared with other unsupervised representation learning approaches, such as VAEs [27], BiGAN [28], AVFs do not need to learn an explicit encoder. Compared with self-supervised learning approaches, such as [29, 30, 31, 32], our approach is density estimation based, and do not need any domain specific priors to create self supervision signal.

5 Experiments

5.1 Setup

We conduct our experiments on images of size 32×32 , using CIFAR10 and CIFAR100 [33], CelebA [34] and ImageNet [35]. Our architecture is a re-implementation of the architecture used in [23], with the addition of Spectral Normalization (SN) [24] to the discriminator weights, and a final Sigmoid

Table 1: Evaluating feature extraction techniques w.r.t. classification accuracy on CIFAR10 with a linear classifier. Here AFV-k-n denotes AFV trained with model channel size k and with n examples. D-pool corresponds to using the pooled features from four layers using the same discriminator as in AFV-128-50000. When using linear classifiers on top of pre-trained features, AFV outperforms state-of-the-art classifiers by a large margin. Remarkably, the classification accuracy increases as we add more data, either in the form of data augmentation or even out of distribution data (CIFAR100) during the GAN training phase.

Method	CIFAR10	CIFAR100	Method	#Features
Exemplar CNN [29]	84.3	-	Unsupervised	-
DCGAN [38]	82.8	-	Unsupervised	-
Deep Infomax [39]	75.6	47.7	Unsupervised	1024
RotNet Linear [30]	81.8	-	Self-Supervised	~25K
AET Linear [32]	83.3	-	Self-Supervised	~25K
D-pool-128-50000	65.3	-	Unsupervised	1.5M
AFV-128-50000	86.2	-	Unsupervised	1.5M
AFV-128-50000 + augment	87.1	-	Unsupervised	1.5M
AFV-256-50000 + augment	88.5	-	Unsupervised	5.9M
AFV-256-50000 + C100 + augment	89.1	67.8	Unsupervised	5.9M
D + BN supervised training	92.7	70.3	Supervised	-

nonlinearity to the discriminator. We adopt the least squares loss as proposed in LSGAN [36] as the default loss for the discriminator, and use the squared loss version of Equation 7 for the generator, with $\gamma = 0$. Unless otherwise mentioned, the channel size for convolutional layers is 128. All experiments use batch size 64, ADAM optimizer [37] with $\beta_1 = 0$, $\beta_2 = .999$, learning rate for $G = 2 \times 10^{-4}$, and learning rate for $D = 4 \times 10^{-4}$. By default we train our model with a fixed number of iterations (800K) and obtain the last checkpoint for evaluation, unless otherwise mentioned.

5.2 Evaluating AFV representations

An appealing property of the EBM view of GAN training is that the discriminator should be able to learn a density function that characterizes the data manifold of the training set. This is in stark contrast to GAN theory, where D reduces to a constant function at convergence. To verify the usefulness of a trained discriminator, we trained a set of models with different settings and compute the AFVs for the dataset. To be concrete, we start from the default architecture and experiment with adding data augmentation, increasing the size of the model by using 256 channels for both D and G and combining CIFAR10 and CIFAR100. We then train a linear classifier with squared hinge loss (L2SVM) on the extracted features to focus on the direct quality of the feature representation as opposed to the power of the classifier. We obtain a state-of-the-art unsupervised pretraining classification accuracy of 89.1% and 67.8 on CIFAR10 and CIFAR100, respectively, as shown in Table 1. These results are also comparable to the supervised learning result with the discriminator’s architecture (while replacing Spectral Normalization with Batch Normalization for better performance, shown in the last row). In contrast, a control experiment without data augmentation shows that pooling D features is significantly worse than the extracted AFV representation on CIFAR10 (65.3% vs. 86.2%). In addition, we show in Figure 2 that the AFVs successfully recover a semantically intuitive notion of similarity between classes (e.g., cars are similar to trucks, dogs are similar to cats). Notably, the dimensionality of our AFVs is 3 orders of magnitude higher than those of the existing methods, which would typically bring a higher propensity to overfitting. However, AFVs still show great generalization ability, demonstrating that they are indeed capturing a meaningful low dimensional subspace that allows easy interpolation between examples. See Supplementary Figures 6 and 7 for visualizations of nearest neighbors.

While AFVs capture properties of the data manifold useful for classification and comparing samples, they may contain additional fine-grained perceptual information. Therefore, in our final experiment we examine the usefulness of AFVs as a perceptual similarity metric consistent with human judgments. Following the approach described in [40], we use the AFV representation to compute distances between image patches and compare with existing methods on the Berkeley-Adobe Perceptual Patch Similarity (BAPPS) dataset on 2AFC and Just Noticeable Difference (JND) metrics. We first train a GAN on ImageNet with the same architecture and settings as previous experiments, and then calculate AFVs on the BAPPS evaluation set. Table 2 shows the performance of AFV along with

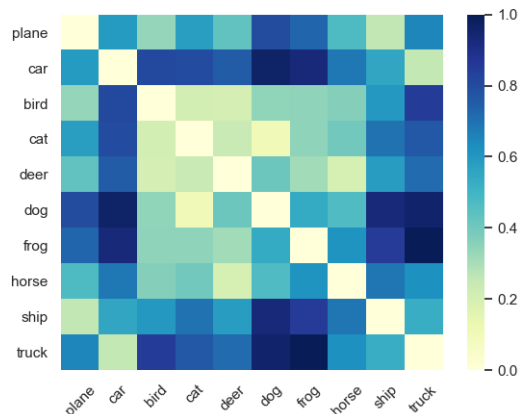


Figure 2: The class distance matrix derived by computing the Fisher Distance between sets of examples representing each class. We see that although trained in an unsupervised way, the Fisher Vectors for each class (set of images) effectively capture semantic similarities between classes.

Table 2: 2AFC and JND scores for different models across traditional and CNN distortion benchmarks reported in [40]. The first three methods are supervised (top). The second two methods are self-supervised (middle). The last two methods, including AFV, are unsupervised (bottom).

Model	2AFC (trad)	2AFC (CNN)	Avg 2AFC	JND (trad)	JND (CNN)	Avg JND
AlexNet [41]	70.6	83.1	76.8	44.0	67.1	55.6
SqueezeNet [42]	73.3	82.6	78.0	49.3	67.6	58.4
VGG [43]	70.1	81.3	75.7	47.5	67.1	57.3
Puzzle [31]	71.5	82.0	76.8	-	-	-
BiGAN [28]	69.8	83.0	76.4	-	-	-
Stacked K-means [44]	66.6	83.0	74.8	-	-	-
AFV (ours)	74.9	80.2	77.6	55.7	62.0	58.9

a variety of existing benchmarks, averaging across traditional and CNN-based distortion sets as in [40]. AFV exceeds the reported unsupervised and self-supervised methods and is competitive with supervised methods trained on ImageNet. Crucially, AFV is domain-independent, and does not require label-based supervision for training the features or the perceptual similarity metric.

5.3 Using the Fisher Distance to monitor training

One of the difficulties of GAN training is the lack of reliable metrics, e.g., a bounded loss function. Recently, domain specific methods, such as Inception Scores (IS) [7] and Fréchet Inception Distance (FID) [45] have been used as surrogate metrics to monitor the quality of generated examples. However, such scores usually rely on a discriminative model trained on ImageNet, and thus have limited applicability to datasets that are drastically different. In this section, we show that monitoring the Fisher Distance between the set of real and generated examples serves as an informative tool to diagnose the training process. To this end, we conducted a set of experiments on CIFAR10 by varying the number of training examples from the set $\{1000, 5000, 25000, 50000\}$. Figure 3 shows the batch-wise estimate of IS and the "Fisher Similarity", which is defined as $e^{-\lambda \mathcal{D}(\mathbf{X}_r, \mathbf{X}_g)}$. Here \mathbf{X}_r and \mathbf{X}_g denotes a batch of real and generated examples, respectively; λ is a temperature term which we set as 10.

We see that when the number of training examples is large, the validation Fisher Similarity steadily increases, aligning with Inception Score. On the other hand, when the number of training examples is small, the validation Fisher Similarity starts decreasing at some point. The model then stops learning, where the corresponding Inception Score also saturates. One caveat about using the Fisher Distance is that the score is generally only comparable within the same training run, as the approximation of the Fisher Information is not accurate and the Fisher Information is not invariant under reparameterization.

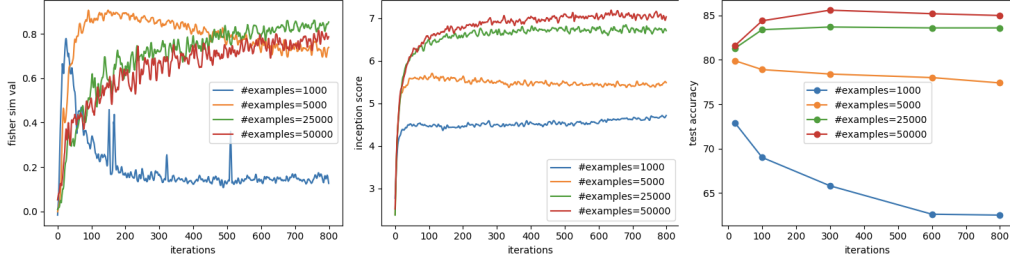


Figure 3: Fisher Similarity of the validation set (left), Inception Scores (middle) by varying the number of training examples from $\{1000, 5000, 25000, 50000\}$, classification test accuracy with AFVs obtained at various checkpoints (right). We see that while the absolute values of the Fisher Similarities are not comparable across models, the trend of the progression of the Fisher Similarities are indicative of optimization and overfitting, which correlates well with the classification accuracy, while the Inception Score fails to do so.

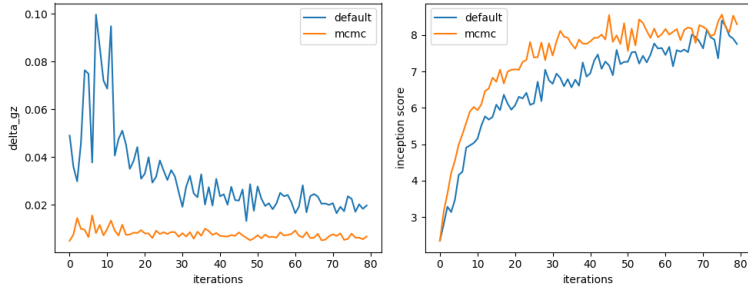


Figure 4: Left: $\Delta G(\mathbf{z})$ of the default generator objective and Equation 7 for the first 80K iterations. Right: the corresponding Inception Scores. In the early phases of training, the MCMC objective maintains small local updates of the generated samples, which results in faster and more stable training.

However, empirically we have found that increasing validation Fisher Similarity is a good indicator of training progress and generalization to unseen data. To support this, we obtained 5 checkpoints from the 4 models at iteration 20, 100, 300, 600, 800, respectively, and trained an L2SVM with the corresponding AFVs, where we show that the classification accuracy correlates well with the validation Fisher Similarity (right panel of Figure 3). The Inception Score does not capture the observed overfitting.

5.4 Interpreting G update as parameterized MCMC

One necessary condition for applying AFV is assuming that the generator is approximating the EBM well during the course of training. To test this hypothesis, we trained a model on ImageNet with size 64×64 , and accordingly modify the default architecture by adding one residual block to both the generator and discriminator. We compare the default generator objective and the MCMC objective in Equation 7 in Figure 4, where we show the training statistics in the first 80K iterations. We monitor $\Delta(G(\mathbf{z}))$, namely the change of generated examples after one G update, which corresponds to the second term of Equation 7. We see that with the explicit MCMC objective, $\Delta G(\mathbf{z})$ maintains a small quantity always, which also results in an improvement in Inception score over the default objective. Supplementary Figure 8 shows a comparison of generated sample quality when training with and without the MCMC objective. We hypothesize that local updates of G can be achieved via architecture search and learning schedule tuning, but in practice, we have found that using the MCMC objective with a small γ often times yield faster training than the standard G losses, especially in the early training phases.

6 Conclusion

In this paper, we demonstrated that GANs can be reinterpreted in order to learn representations that have desirable qualities for a diverse set of tasks without requiring domain knowledge or labeled data. We showed that a well trained GAN can capture the intrinsic manifold of data and be used for density estimation following the AFV methodology. We provided empirical analysis supporting the strength of our method. First, we showed that AFVs are a reliable indicator of whether GAN training is well behaved, and that we can use this monitoring to select good model checkpoints. Second, we showed that forcing the generator to track MCMC improves stability and leads to better density models. We next showed that AFVs are a useful feature representation for linear and nearest neighbor classification, achieving state-of-the-art among unsupervised feature representations on CIFAR-10. Finally, we showed that a well-trained GAN discriminator does contain useful information for fine-grained perceptual similarity. Taken together, these experiments show the usefulness of the EBM and associated Fisher Information framework for extracting useful representational features from GANs. In future work, we plan to improve the scalability of the AFV method by compressing the Fisher Vector representation, e.g., using product quantization as in [11].

References

- [1] Ian Goodfellow, Jean Pouget-Abadie, Mehdi Mirza, Bing Xu, David Warde-Farley, Sherjil Ozair, Aaron Courville, and Yoshua Bengio. Generative adversarial nets. In *Advances in neural information processing systems*, pages 2672–2680, 2014.
- [2] Taesup Kim and Yoshua Bengio. Deep directed generative models with energy-based probability estimation. *arXiv preprint arXiv:1606.03439*, 2016.
- [3] Shuangfei Zhai, Yu Cheng, Rogerio Feris, and Zhongfei Zhang. Generative adversarial networks as variational training of energy based models. *arXiv preprint arXiv:1611.01799*, 2016.
- [4] Dilin Wang and Qiang Liu. Learning to draw samples: With application to amortized mle for generative adversarial learning. *arXiv preprint arXiv:1611.01722*, 2016.
- [5] Tommi Jaakkola and David Haussler. Exploiting generative models in discriminative classifiers. In *Advances in neural information processing systems*, pages 487–493, 1999.
- [6] Max Welling and Yee W Teh. Bayesian learning via stochastic gradient langevin dynamics. In *Proceedings of the 28th international conference on machine learning (ICML-11)*, pages 681–688, 2011.
- [7] Tim Salimans, Ian Goodfellow, Wojciech Zaremba, Vicki Cheung, Alec Radford, and Xi Chen. Improved techniques for training gans. In *Advances in neural information processing systems*, pages 2234–2242, 2016.
- [8] Sergey Ioffe and Christian Szegedy. Batch normalization: Accelerating deep network training by reducing internal covariate shift. *arXiv preprint arXiv:1502.03167*, 2015.
- [9] Shun-Ichi Amari. Natural gradient works efficiently in learning. *Neural computation*, 10(2):251–276, 1998.
- [10] Shun-ichi Amari and Hiroshi Nagaoka. *Methods of information geometry*, volume 191. American Mathematical Soc., 2007.
- [11] Jorge Sánchez, Florent Perronnin, Thomas Mensink, and Jakob Verbeek. Image classification with the fisher vector: Theory and practice. *International Journal of Computer Vision*, 105(3):222–245, Dec 2013.
- [12] Geoffrey E Hinton. A practical guide to training restricted boltzmann machines. In *Neural networks: Tricks of the trade*, pages 599–619. Springer, 2012.
- [13] Ian Goodfellow, Yoshua Bengio, and Aaron Courville. *Deep learning*. MIT press, 2016.
- [14] Yilun Du and Igor Mordatch. Implicit generation and generalization in energy-based models. *arXiv preprint arXiv:1903.08689*, 2019.
- [15] Junbo Zhao, Michael Mathieu, and Yann LeCun. Energy-based generative adversarial network. *arXiv preprint arXiv:1609.03126*, 2016.

- [16] Martin Arjovsky, Soumith Chintala, and Léon Bottou. Wasserstein gan. *arXiv preprint arXiv:1701.07875*, 2017.
- [17] Sebastian Nowozin, Botond Cseke, and Ryota Tomioka. f-gan: Training generative neural samplers using variational divergence minimization. In *Advances in neural information processing systems*, pages 271–279, 2016.
- [18] Chun-Liang Li, Wei-Cheng Chang, Yu Cheng, Yiming Yang, and Barnabás Póczos. Mmd gan: Towards deeper understanding of moment matching network. In *Advances in Neural Information Processing Systems*, pages 2203–2213, 2017.
- [19] Yann LeCun, Sumit Chopra, and Raia Hadsell. A tutorial on energy-based learning. *yann.lecun.com*, 2006.
- [20] Yilun Du and Igor Mordatch. Implicit generation and generalization in energy-based models. *arXiv preprint arXiv:1903.08689*, 2019.
- [21] Erik Nijkamp, Mitch Hill, Tian Han, Song-Chun Zhu, and Ying Nian Wu. On the anatomy of mcmc-based maximum likelihood learning of energy-based models. *arXiv preprint arXiv:1903.12370*, 2019.
- [22] Kevin Roth, Aurélien Lucchi, Sebastian Nowozin, and Thomas Hofmann. Stabilizing training of generative adversarial networks through regularization. *CoRR*, abs/1705.09367, 2017.
- [23] Ishaan Gulrajani, Faruk Ahmed, Martin Arjovsky, Vincent Dumoulin, and Aaron C Courville. Improved training of wasserstein gans. In *Advances in Neural Information Processing Systems*, pages 5767–5777, 2017.
- [24] Takeru Miyato, Toshiki Kataoka, Masanori Koyama, and Yuichi Yoshida. Spectral normalization for generative adversarial networks. In *International Conference on Learning Representations*, 2018.
- [25] Lars Mescheder, Andreas Geiger, and Sebastian Nowozin. Which training methods for gans do actually converge? *arXiv preprint arXiv:1801.04406*, 2018.
- [26] Alessandro Achille, Michael Lam, Rahul Tewari, Avinash Ravichandran, Subhansu Maji, Charles Fowlkes, Stefano Soatto, and Pietro Perona. Task2vec: Task embedding for meta-learning. *arXiv preprint arXiv:1902.03545*, 2019.
- [27] Diederik P Kingma and Max Welling. Auto-encoding variational bayes. *arXiv preprint arXiv:1312.6114*, 2013.
- [28] Jeff Donahue, Philipp Krähenbühl, and Trevor Darrell. Adversarial feature learning. *CoRR*, abs/1605.09782, 2016.
- [29] Alexey Dosovitskiy, Philipp Fischer, Jost Tobias Springenberg, Martin Riedmiller, and Thomas Brox. Discriminative unsupervised feature learning with exemplar convolutional neural networks. *IEEE transactions on pattern analysis and machine intelligence*, 38(9):1734–1747, 2015.
- [30] Spyros Gidaris, Praveer Singh, and Nikos Komodakis. Unsupervised representation learning by predicting image rotations. *arXiv preprint arXiv:1803.07728*, 2018.
- [31] Mehdi Noroozi and Paolo Favaro. Unsupervised learning of visual representations by solving jigsaw puzzles. *CoRR*, abs/1603.09246, 2016.
- [32] Liheng Zhang, Guo-Jun Qi, Liqiang Wang, and Jiebo Luo. Aet vs. aed: Unsupervised representation learning by auto-encoding transformations rather than data. *arXiv preprint arXiv:1901.04596*, 2019.
- [33] A. Krizhevsky and G. Hinton. Learning multiple layers of features from tiny images. *Master’s thesis, Department of Computer Science, University of Toronto*, 2009.
- [34] Ziwei Liu, Ping Luo, Xiaogang Wang, and Xiaoou Tang. Deep learning face attributes in the wild. In *Proceedings of International Conference on Computer Vision (ICCV)*, 2015.
- [35] J. Deng, W. Dong, R. Socher, L.-J. Li, K. Li, and L. Fei-Fei. ImageNet: A Large-Scale Hierarchical Image Database. In *CVPR09*, 2009.
- [36] Xudong Mao, Qing Li, Haoran Xie, Raymond YK Lau, Zhen Wang, and Stephen Paul Smolley. Least squares generative adversarial networks. In *Proceedings of the IEEE International Conference on Computer Vision*, pages 2794–2802, 2017.

- [37] Diederik P. Kingma and Jimmy Ba. Adam: A method for stochastic optimization. In *3rd International Conference on Learning Representations, ICLR 2015, San Diego, CA, USA, May 7-9, 2015, Conference Track Proceedings*, 2015.
- [38] Alec Radford, Luke Metz, and Soumith Chintala. Unsupervised representation learning with deep convolutional generative adversarial networks. *arXiv preprint arXiv:1511.06434*, 2015.
- [39] R Devon Hjelm, Alex Fedorov, Samuel Lavoie-Marchildon, Karan Grewal, Phil Bachman, Adam Trischler, and Yoshua Bengio. Learning deep representations by mutual information estimation and maximization. *arXiv preprint arXiv:1808.06670*, 2018.
- [40] Richard Zhang, Phillip Isola, Alexei A. Efros, Eli Shechtman, and Oliver Wang. The unreasonable effectiveness of deep features as a perceptual metric. *CoRR*, abs/1801.03924, 2018.
- [41] Alex Krizhevsky, Ilya Sutskever, and Geoffrey E Hinton. Imagenet classification with deep convolutional neural networks. In F. Pereira, C. J. C. Burges, L. Bottou, and K. Q. Weinberger, editors, *Advances in Neural Information Processing Systems 25*, pages 1097–1105. Curran Associates, Inc., 2012.
- [42] Forrest N. Iandola, Matthew W. Moskewicz, Khalid Ashraf, Song Han, William J. Dally, and Kurt Keutzer. Squeezenet: Alexnet-level accuracy with 50x fewer parameters and <1mb model size. *CoRR*, abs/1602.07360, 2016.
- [43] K. Simonyan and A. Zisserman. Very deep convolutional networks for large-scale image recognition. In *International Conference on Learning Representations*, 2015.
- [44] Philipp Krähenbühl, Carl Doersch, Jeff Donahue, and Trevor Darrell. Data-dependent initializations of convolutional neural networks. *arXiv preprint arXiv:1511.06856*, 2015.
- [45] Martin Heusel, Hubert Ramsauer, Thomas Unterthiner, Bernhard Nessler, and Sepp Hochreiter. Gans trained by a two time-scale update rule converge to a local nash equilibrium. In *Advances in Neural Information Processing Systems*, pages 6626–6637, 2017.

7 Supplementary Material

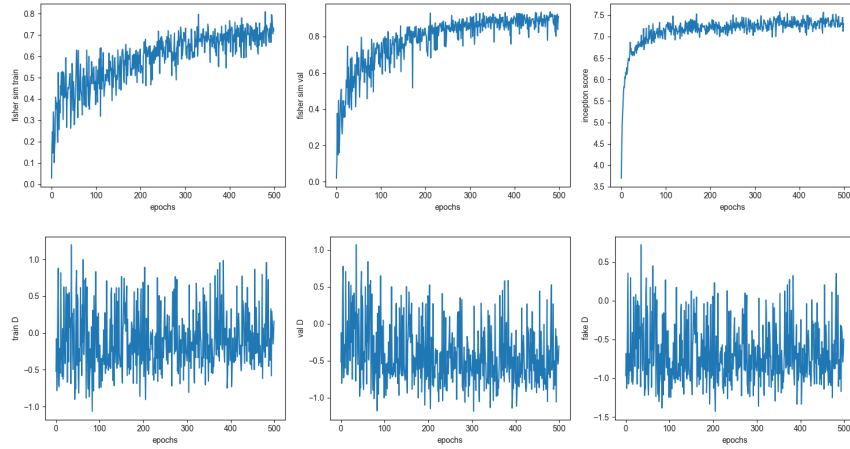


Figure 5: Progression of various statistics during the course of training a healthy GAN on CIFAR10. From top left to bottom right: training Fisher Similarity, validation Fisher Similarity, Inception Score, training discriminator score, validation discriminator score, generated discriminator score. We see that both the training and validation Fisher Similarity correlates well with Inception Score, healthily increasing. The discriminator’s scores on the other hand do not exhibit a clear pattern.

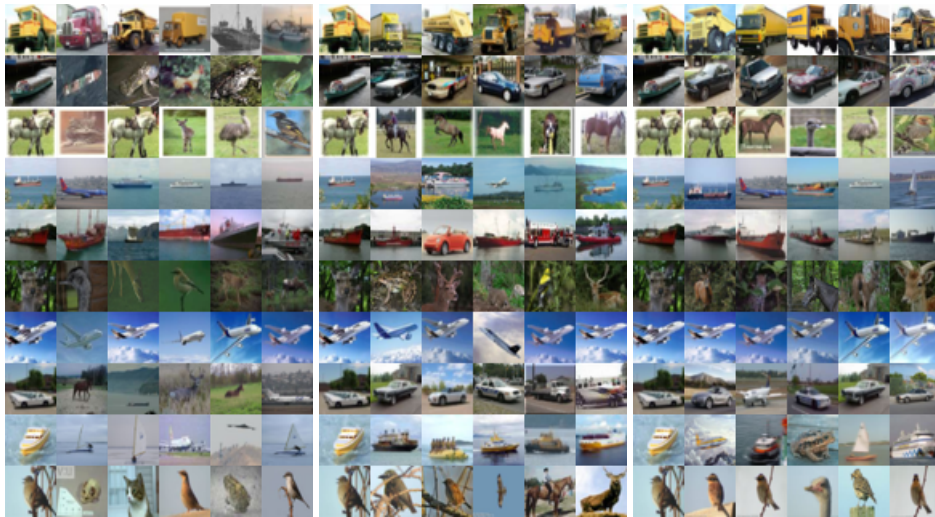


Figure 6: Visualization of 5 nearest training examples of 10 **test** examples using pixel (left), ResNet18 (middle) and Fisher vector representations (right), respectively. In each block, the leftmost column shows test examples, while the remaining five columns show the retrieved 5 nearest neighbors, sorted by the distance.



Figure 7: Left: Five nearest generated examples (column 2 to 5 in each row) of a given **training** example (column 1 in each row). Right: Five nearest training examples (column 2 to 5 in each row) of a given **generated** example (column 1 in each row). Both plots are generated with the Fisher Distance.

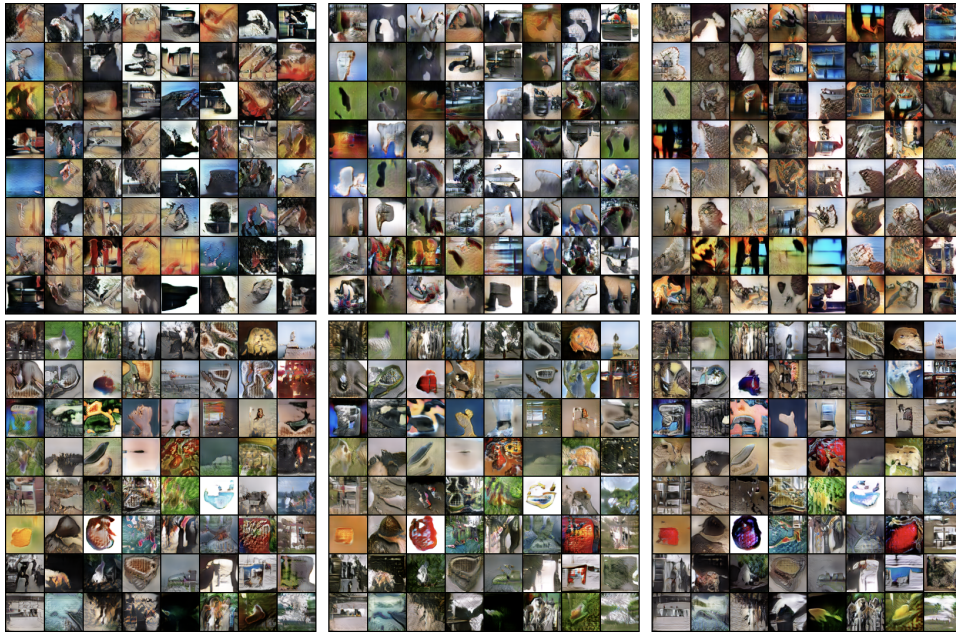


Figure 8: Generated samples in the early training phase (after 10K, 11K and 12K iterations, from left to right). Top: samples from using the default G update. Bottom: samples generated using using the MCMC objective in Equation 7 with $\lambda = 1$. Note how with the MCMC objective, samples change gradually (compare same patch position across the three training checkpoints) and exhibit better quality and diversity at the same time, with fewer artifacts. (Best viewed in high resolution)